SCISPACE
formerly Typeset

Open access • Journal Article • DOI:10.1524/ZKRI.2008.1124

Hydrogen induced site depopulation in the LaMgNi4-hydrogen system

— Source link

Jean-Noël Chotard, Denis Sheptyakov, Klaus Yvon

Published on: 01 Oct 2008 - Zeitschrift Fur Kristallographie (Oldenbourg Wissenschaftsverlag GmbH)

Topics: Hydride, Hydrogen and Interstitial defect

Related papers:

- Synthesis, crystal structure and hydrogenation properties of the ternary compounds LaNi4Mg and NdNi4Mg
- Structural and hydriding properties of MgYNi4:: A new intermetallic compound with C15b-type Laves phase structure
- Structural determination of AMgNi4 (where A=Ca, La, Ce, Pr, Nd and Y) in the AuBe5 type structure
- X-ray/neutron diffraction studies and ab initio electronic structure of CeMgNi4 and its hydride
- Hydrogen storage properties of new ternary system alloys: La2MgNi9, La5Mg2Ni23, La3MgNi14

Share this paper:

View more about this paper here: https://typeset.io/papers/hydrogen-induced-site-depopulation-in-the-lamgni4-hydrogen-15k7t9chd3

ETH zürich

ETH Library

Hydrogen induced site depopulation in the LaMgNi4-hydrogen system

Journal Article

Author(s):
Chotard, Jean-Noël; Sheptyakov, Denis; Yvon, Klaus

Publication date:
2009

Permanent link:
https://doi.org/10.3929/ethz-b-000013669

Rights / license:
In Copyright - Non-Commercial Use Permitted

Originally published in:
Zeitschrift für Kristallographie 223(10), https://doi.org/10.1524/zkri.2008.1124

This page was generated automatically upon download from the ETH Zurich Research Collection.
For more information, please consult the Terms of use.

Z. Kristallogr. **223** (2008) 690–696 / **DOI** 10.1524/zkri.2008.1124
© by Oldenbourg Wissenschaftsverlag, München

Hydrogen induced site depopulation in the $LaMgNi_4$-hydrogen system

Jean-Noël Chotard*,[I], Denis Sheptyakov[II] and Klaus Yvon[I]

[I] Laboratoire de Cristallographie, Université de Genève, Switzerland
[II] Laboratory for Neutron Scattering ETH Zurich & PSI Villigen, Switzerland

Received August 6, 2008; accepted October 30, 2008

Metal hydride structures / In-situ neutron powder diffraction / Pressure-composition-isotherms / Structure-property relation

Abstract. The $LaMgNi_4$-hydrogen system was investigated by in-situ neutron powder diffraction and pressure-composition isotherm measurements at 100 °C and hydrogen (deuterium) pressures of up 50 bar. The system displays three hydride phases that have distinctly different hydrogen plateau pressures and H atom distributions. The cubic α-$LaMgNi_4H_{0.75}$ phase forms below 0.01 bar hydrogen pressure and H atoms fill one type of tetrahedral Ni_4 interstices. The orthorhombic distorted β-$LaMgNiH_{3.7}$ phase forms at ~3 bar hydrogen pressure and H atoms fill both tetrahedral $LaNi_3$ and triangular bi-pyramidal La_2MgNi_2 interstices. Interestingly, tetrahedral Ni_4 interstices are no longer occupied. Finally, the most hydrogen rich γ-$LaMgNi_4H_{4.85}$ phase forms above 20 bar. It has again cubic symmetry and H atoms continue to occupy triangular bi-pyramidal La_2MgNi_2 interstices while filling a new type of tetrahedral Ni_4 interstices that are neither occupied in the α- nor in the β-phase. The tetrahedral $LaNi_3$ interstices occupied in the β-phase are empty. Hydrogen induced depopulations of interstitial sites in metal hydrides are relatively rare and consistent with, but not entirely due to, the onset of repulsive H–H interactions at increasing hydrogen concentrations.

Introduction

The La–Mg–Ni–H system is subject of numerous studies that are motivated by the discovery of superior electrochemical properties of Mg containing compositions compared to Mg free compositions [1]. These studies have identified the intermetallic compounds $(La,Mg)_2Ni_7$ and $LaMgNi_4$ as active phases in electrodes for use in rechargeable metal hydride batteries (see for example [2] and references therein), and their properties have been examined by many authors (see for example [3–5] and references therein). Further interest in the La–Mg–Ni–H system was recently raised by our discovery of hydrogen induced metal-insulator (M-I) transitions for compositions such as $LaMg_2Ni$–H [6] and La_2MgNi_2–H [7]. In view of this work, we decided to investigate a system having the composition $LaMgNi_4$–H. The intermetallic compound $LaMgNi_4$ is known [8, 9] to crystallize with the cubic $MgCu_4Sn$ type structure, an ordered derivative of the well known cubic Laves phase (C15) type structure. In a previous study [10] we have reported ex-situ structure and pressure-composition isotherm (PCI) data for the analogous neodymium system $NdMgNi_4$–H which contains a hydride phase that is stable at room temperature but looses hydrogen rapidly in air. Useful data for the lanthanum analogue $LaMgNi_4$–H, however, were not obtained because the system tended to segregate during hydrogenation. Here we report PCI measurements and in-situ neutron powder diffraction data for this system at 100 °C and hydrogen (deuterium) pressures of up to 50 bar. It will be shown that under these conditions the $LaMgNi_4$–H system displays at least three well defined hydride phases in which hydrogen fills metal interstices in a way that differs significantly from the closely related C15 type metal-hydrogen systems. Furthermore, the system shows a depopulation of hydrogen sites as a function of hydrogen concentration which is an unexpected and relatively rare phenomenon in transition metal hydrides.

Experimental

Synthesis

Samples of nominal composition $LaMgNi_4$ were prepared in several steps. Mixtures of lanthanum ingots and compressed nickel powder were first arc melted several times to increase homogeneity. The resulting "$LaNi_4$" pellets were then grinded in a glove box under argon atmosphere and magnesium powder was added. The mixtures were then pressed into new pellets, wrapped into tantalum foils and placed in stainless steel tubes that were sealed by arc melting in the glove box under argon atmosphere. The steel tubes were previously cleaned with nitric and acetic acid. Finally, the tubes were introduced into a tubular furnace and heated under the following conditions: 36 hours at 450 °C, 4 hours at 620 °C and 36 hours at 720 °C. The

* Correspondence author (e-mail: jean-noel.chotard@cryst.unige.ch)

tubes were then slowly cooled down to room temperature and opened in air. X-ray powder diffraction (XPD) on a laboratory instrument (Bruker D8 Advance) revealed the presence of quasi single-phase samples that consisted mainly of the known cubic $LaMgNi_4$ phase [9] and small quantities (<1 wt%) of the hexagonal $LaNi_5$ phase, but no oxide was identified. Rietveld refinements from X-ray powder diffraction yielded structure parameters for the $LaMgNi_4$ phase similar to those reported previously [9], except for the cubic cell parameter that was intermediate between those reported ($a = 7.17027(1)$ Å, as compared to $a = 7.1794(2)$ Å reported in [9] and 7.165(1) Å in [11]) and the positional parameter of Ni that was refined rather than fixed ($x = 0.6240(1)$, as compared to $x = 0.625(-)$ in [9]). Before performing in-situ neutron powder diffraction (NPD) and pressure-composition isotherm (PCI) measurements, the samples were activated under dynamic vacuum ($3 \cdot 10^{-2}$ mbar) at 120 °C overnight and then charged at 100 °C with hydrogen (for the PCI measurement) or deuterium (for the NPD measurement) at pressures of up to 50 bar. The hydrides showed no sign of pyrophoricity but tended to decompose in air by catalytic water formation.

Neutron powder diffraction and structure refinement

A $LaMgNi_4$ sample of ~5 g mass was used for data collection on a high-resolution powder diffractometer (HRPT at SINQ, PSI, Villigen) in the high intensity mode by using various wavelengths ($\gamma = 1.1545$, 1.4940, 1.8857 Å) and 2θ ranges (5–164°, step size 0.1°). The in-situ measurements were carried out at 100 °C by placing the sample into a steel container (diameter: 8 mm, length: 50 mm, wall thickness 1 mm) that was filled at about 60% and connected to a pressurized deuterium bottle. Exploratory data sets were collected at 0, 1, 2, 5 (±1) and 10 (±1) bar deuterium pressure at 100 °C, revealing the presence of at least two deuteride phases (α and β). The sample was then desorbed at 130 °C under dynamic vacuum ($3 \cdot 10^{-3}$ mbar) and investigated by XRD. The patterns showed that the sample had totally desorbed but was still well crystallized. In a second step, a series of in-situ NPD data were collected at 100 °C on the desorbed sample in order to explore the conditions for obtaining the various deuteride phases in pure form. To do so, the deuterium pressure was increased from vacuum to 2 bar and then in steps of ~5 bar up to 52 (±1) bar, and at each step data were collected for at least 30 minutes while deuteration took place. From these (quasi dynamic) measurements the α- and β-phases were found to start forming at ~2 bar and ~10 (±1) bar, respectively, while a third phase (γ) was found to start forming at ~44 (±1) bar. On the other hand, whenever the deuterium absorption slowed down significantly, or nearly stopped, the data collection time was increased to up to 7 hours. From these (quasi-static) measurements three diffraction patterns were obtained whose quality was sufficient for structure analyses (pattern 1 recorded at 5 (±1) bar, pattern 2 at 10 (±1) bar, pattern 3 at 52 (±1) bar). The patterns were indexed by the program DICVOL04 [12] when necessary and the D atoms were located by the program FOX [13]. The structure refinements were carried out by using the FULLPROF SUITE program package [14]. Refined diffraction patterns are shown in Fig. 1, and structure data and refinement indices for the three deuteride phases are summarized in Table 1. Besides the majority phases α, β, γ all patterns showed the presence of secondary phases (pattern 1: 11.5 wt% of β-$LaMgNi_4MgD_x$; pattern 2: 12.0 wt% of α-$LaMgNi_4D_x$, pattern 3: 4.8 wt% of $LaNi_5$) and strong contributions due to the stainless steel container (modeled by a face centered cubic lattice having $a = 3.60152$ Å). However, in view of the low abundances, reliable structure parameters for the secondary phases could not be obtained. On the other hand, the apparent absence of

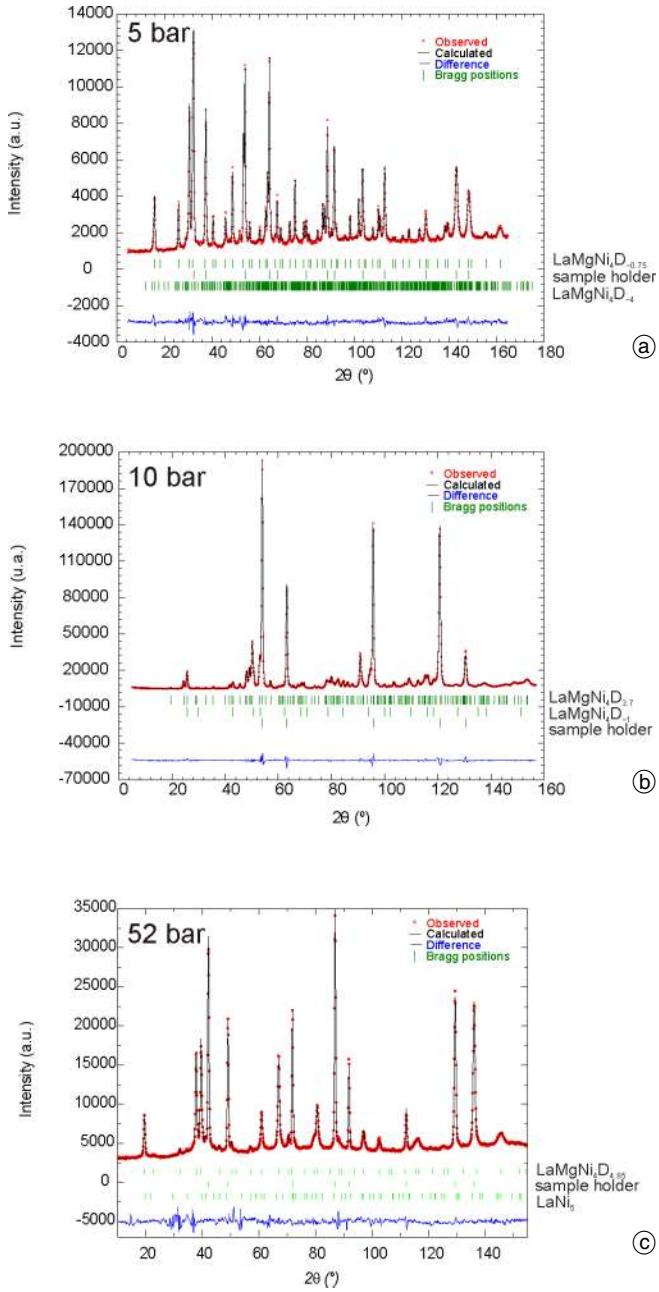

Fig. 1. Observed and calculated in-situ neutron powder diffraction patterns of $LaMgNi_4Mg-D$ system at 100 °C at 5 bar (**a**), 10 bar (**b**) and 52 bar (**c**) deuterium pressure. Majority phases in patterns a–c are α-$LaMgNi_4MgD_{0.75}$ ($\lambda = 1.1545$ Å), β-$LaMgNi_4MgD_{3.7}$ ($\lambda = 1.8857$ Å) and γ-$LaMgNi_4MgD_{4.85}$ ($\lambda = 1.494$ Å), respectively; phases are indicated by markers.

Table 1. Crystal structure data and refinement indices for $LaMgNi_4D_x$ phases as obtained from neutron powder diffraction patterns at deuterium pressures of $p(D_2) = 5$ bar (pattern 1), 10 bar (pattern 2) and 52 bar (pattern 3) at $T = 100$ °C; e.s.d.'s in parentheses.

α-$LaMgNi_4D_{0.75}$: space group $F\bar{4}3m$, $a = 7.27871(2)$ Å, $V = 385.62(1)$ Å^3, $Rp = 0.115$, $Rwp = 0.108$, $R_{Bragg} = 0.063$, $\chi^2 = 5.12$. Secondary phase: 11.5 wt% of β-$LaMgNi_4MgD_{3.7}$. $p(D_2) = 5$ bar.

Atom	Wyckoff position	x	y	z	B_{iso}	Occupancy
La	4*a*	0	0	0	0.87(8)	1
Ni	16*e*	0.6208(3)	0.6208(3)	0.6208(3)	1.47(3)	1
Mg	4*c*	1/4	1/4	1/4	2.7(3)	1
D1	4*d*	3/4	3/4	3/4	2.66(19)	0.75(2)

β-$LaMgNi_4D_{3.7}$: space group $Pmn2_1$, $a = 5.12570(4)$ Å, $b = 5.52436(4)$ Å, $c = 7.45487(4)$ Å, $V = 211.09(2)$ Å^3, $Rp = 0.060$, $Rwp = 0.066$, $R_{Bragg} = 0.027$, $\chi^2 = 14.7$. Secondary phase: 12.0 wt% of α-$LaMgNi_4MgD_{0.75}$. $p(D_2) = 10$ bar.

Atom	Wyckoff position	x	y	z	B_{iso}	Occupancy
La	2*a*	0	0.3044(19)	0	0.1(2)	1
Mg	2*a*	0	0.805(3)	0.2334(19)	0.9(3)	1
Ni1	2*a*	0	0.4537(14)	0.6210(16)	1.07(17)	1
Ni2	2*a*	0	0.9994(17)	0.6084(16)	1.36(18)	1
Ni3	4*b*	0.7512(15)	0.2247(11)	0.3812(11)	0.76(9)	1
D1	4*b*	0.7600(17)	0.5146(17)	0.7598(18)	1.2(4)	0.84(3)
D2	2*a*	0	0.726(3)	0.514(2)	2.8(3)	1
D3	2*a*	0	0.931(2)	0.8188(19)	2.4(3)	1

γ-$LaMgNi_4D_{4.85}$: space group $F\bar{4}3m$, $a = 7.65840(4)$ Å, $b = 7.65840(4)$ Å, $c = 7.65840(4)$ Å, $V = 449.17(3)$ Å^3, $Rp = 0.094$, $Rwp = 0.078$, $R_{Bragg} = 0.022$, $\chi^2 = 4.48$). Secondary phase: 4.8 wt% of $LaNi_5$. $p(D_2) = 52$ bar.

Atom	Wyckoff position	x	y	z	B_{iso}	Occupancy
La	4*a*	0	0	0	2.5(3)	1
Ni	16*e*	0.6194(5)	0.6194(5)	0.6194(5)	2.05(8)	1
Mg	4*c*	1/4	1/4	1/4	4.6(5)	1
D1	24*g*	0.9875(11)	1/4	1/4	2.5(3)	0.72(1)
D2	4*b*	1/2	1/2	1/2	2.6(8)	0.54(6)

deuterium in the $LaNi_5$ phase (pattern 3) can be explained by the fact that the sample had been exposed to deuterium for a period of only ~16 hours which may be too short for activation.

PCI measurements

In order to determine the hydrogen content and thermal stability of the various hydride phases, PCI data were collected during absorption under up to 50 bar hydrogen pressure at 100 °C by using a Sievert's-type apparatus for a total measuring time of 185 hours. The PCI curve obtained exhibits three more-or-less well defined equilibrium plateau pressures (p_{eq}) at 0.01 bar, 2.5 bar and 23 bar (see Fig. 2) consistent with the formation of the α-, β- and γ-phase, respectively. A subsequent decrease in hydrogen pressure to ambient conditions during ~120 hrs at 100 °C caused the sample to desorb hydrogen only partially (release of 1.5 H/formula unit (f.u.)).

Results

As can be seen from the PCI curve shown in Fig. 2 the $LaMgNi_4$–H system contains at least three hydride phases at 100 °C. The α-phase has a relatively low plateau pressure (~10 mbar) and its upper hydrogen content is close to 1 H/f.u. Its structure undergoes a cell expansion of $\Delta V/V = 4.6\%$ at ~0.75 H/f.u. and keeps cubic symmetry (space group $F\bar{4}3m$). As shown in Fig. 3 the hydrogen (deuterium) atoms occupy exclusively tetrahedral Ni_4 type interstices. Their average occupancy (~0.75) corresponds to an overall composition of α-$LaMgNi_4H_{0.75}$. Such a difference is not uncommon in view of the difficulty in

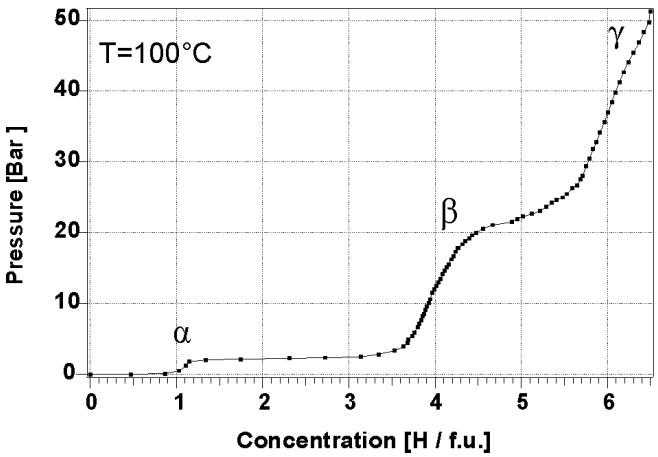

Fig. 2. Pressure-composition-isotherm of $LaMgNi_4$–H system during absorption at 100 °C and approximate upper phase limits (α, β, γ).

phase \ site	24*g*		16*e*	4*b*	4*d*
α	empty		empty	empty	
β				empty	empty
γ	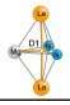		empty		empty

Fig. 3. Population/depopulation sequence of D atom sites and their metal atom environments in the α-, β- and γ-phases of the $LaMgNi_4-D$ system; for occupancies see Table 1; equipoints of D atom sites (24*g*, 16*e*, 4*b*, 4*d*) refer to cubic space group $F\bar{4}3m$ of α- and γ-phase. Trigonal bi-pyramidal interstices of type La_2MgNi_2 (site 24*g*) in β- and γ-phases correspond to pairs of face-sharing tetrahedral interstices of type $LaMgNi_2$ (site 48*h*). Interstices of type $LaMgNi_2$ (48*h*), $LaNi_3$ (16*e*), and Ni_4 (4*d*, 4*b*) correspond to interstices of type A_2B_2 (96*g*), AB_3 (32*e*) and B_4 (8*b*) type interstices, respectively, in C15 type AB_2-H systems ($Fd\bar{3}m$).

reaching equilibrium conditions during in-situ NPD measurements. Likewise, slow kinetics (*i.e.* a sluggish $\alpha-\beta$ phase transformation) presumably also explains why the α-phase has been observed at ~5 bar in the NPD patterns, in contrast to its much lower equilibrium pressure as obtained from PCT data close to equilibrium. The fact that the Ni_4 type interstices are occupied is intriguing. In view of their relatively small size compared to other interstices in the structure, one would expect them to be occupied only at higher hydrogen contents (pressures), in analogy to the tetrahedral B_4 type interstices in AB_2 compounds having C15 type structure (see below).

The more hydrogen rich β-phase forms at ~3 bar hydrogen pressure. Its plateau pressure is relatively flat and extends from ~1.1 to ~4 H/f.u., corresponding to a volume expansion of $V/V \sim 14.5\%$ (at ~3.7 H/f.u. relative to the H-free compound). Similar to the neodymium analogue $NdMgNi_4D_{3.8}$ [10] the structure of this phase is orthorhombic distorted (space group $Pmn2_1$) and displays three new hydrogen (deuterium) sites. One is partially (D1: ~84%) and two others are fully occupied (D2, D3), corresponding to the overall composition β-$LaMgNi_4D_{3.7}$. Interestingly, while one site has the expected tetrahedral coordination (D3: $LaNi_3$), the two other sites have triangular bi-pyramidal (D1, D2: La_2MgNi_2) rather than tetrahedral ($LaMgNi_2$) metal coordinations as in C15 type metal–H systems. As can be seen in Fig. 3, the triangular bi-pyramidal sites are located about half way between the centres of $LaMgNi_2$ tetrahedra sharing faces. Refinements based on a model in which the tetrahedra centres were occupied yielded significantly worse fits to the data. Furthermore, the tetrahedral Ni_4 site originally occupied in the α-phase is no longer occupied in the β-phase. Both features, *i.e.* the shift from tetrahedral towards trigonal bi-pyramidal metal coordination of two D sites, and the depletion of another D site are puzzling. They are presumably related to a variety of factors, including atomic size effects and repulsive interactions between D atoms (see below).

The most hydrogen-rich gamma-phase forms at ~20 bar hydrogen pressure. Its equilibrium plateau in the PCT curve is less well defined and suggests an upper composition of ~6.5 H/f.u. at ~50 bar pressure, corresponding to an estimated volume expansion of ~28% at 6.5 H/f.u. (relative to the H-free compound), and an observed volume expansion of $V/V \sim 21.9\%$ at ~4.85 H/f.u. The fact that the composition of the γ-phase as measured by NPD at 52 bar pressure (~4.85 H/f.u.) is significantly lower than that estimated from the PCT curve (~6.5 H/f.u.) has presumably the same origin as the observed compositional differences in the α-phase (slow kinetics, lack of equilibrium). Interestingly, while the structural symmetry of this phase returns back to cubic (space group $F\bar{4}3m$), the tetrahedral $LaNi_3$ interstices occupied in the β-phase become empty and a new tetrahedral Ni_4 site that is neither occupied in the α-phase nor in the β-phase becomes partially occupied (D2: ~54%, see Fig. 3). On the other hand, the triangular bi-pyramidal La_2MgNi_2 sites continue being occupied (D1: 72%). The refined occupancies suggest an overall composition of γ-$LaMgNi_4D_{4.85}$.

The interatomic distances of the various phases are in the expected ranges. The shortest metal-hydrogen distances are 1.63 Å (Ni) in the α-phase (there are no La–D and Mg–D contacts), 2.46 (La), 2.14 (Mg) and 1.61 (Ni) Å in the β-phase, and 2.71 (La), 2.01 (Mg) and 1.58 (Ni) Å in the γ-phase. As expected, the average metal-metal distances increase with D content and the distances between occupied D atom sites are all >2.1 Å.

Discussion

The $LaMgNi_4-H$ system shows a variety of interesting features. In contrast to its neodymium and yttrium analogues $NdMgNi_4-H$ [10] and $YMgNi_4-H$ [15] it displays at least three hydride phases that have distinctly different hydrogen equilibrium pressures and H atom distributions. While the α- and γ-phases ($p_{eq} < 0.01$ and >20 bar, respectively, at 100 °C) have no analogues in the Nd and Y systems, at least not in the pressure-temperature ranges investigated ($NdMgNi_4-H$ studied up to 4 bar at 50 °C [10]; $YMgNi_4-H$ studied up to 30 bar at 80 °C [15]), β-phases exist in all three systems. That in the La system is thermally more stable than those in the Nd and Y systems (La: $p_{eq} \sim 3$ bar at 100 °C; Nd: $p_{eq} \sim 1-2$ bar at 50 °C; Y: $p_{eq} \sim 20$ bar at 80 °C), as expected from plateau pressure-cell volume correlations observed in metal-hydrogen systems such as AB_5-H (see [16] and references therein).

The structural symmetries and H atom distributions in the $LaMgNi_4-H$ system show unusual trends. Not only does the symmetry change from cubic (α-phase) to orthorhombic (β-phase) and back to cubic again (γ-phase), but the filling sequence of, and the exact hydrogen location within the metal interstices differ from those in the closely related C15 type AB_2-H systems. In the latter hydrogen occupies exclusively tetrahedral A_2B_2, AB_3 and B_4 type interstices made up by relatively large A atoms (*e.g.* lanthanides) and relatively small B atoms (*e.g.* transition- or *p*-elements) [17]. The filling sequence is A_2B_2, AB_3

and B_4 in accordance with atomic size considerations. In the $LaMgNi_4-H$ system, however, hydrogen occupies both tetrahedral and trigonal bi-pyramidal interstices, and the filling sequence is Ni_4 (α-phase), $La_2MgNi_2 + LaNi_3$ (β-phase) and $La_2MgNi_2 + Ni_4$ (γ-phase), as shown in Fig. 3. Deviations from tetrahedral metal coordination in C15-type metal-hydrogen systems have so far only been observed in saline metal hydrides such as tetragonal distorted $LnMg_2H_7$ (Ln = La, Ce [18], Sm [19]) in which hydrogen occupies a site having triangular metal coordination (2Ln, Mg). Furthermore, in contrast to C15 type metal–hydrogen systems there exist various interstices of a given type that are not symmetry equivalent, such as two B_4 type (Ni_4), two AB_3 type ($LaNi_3$, $MgNi_3$) and two A_2B_2 type interstices ($LaMgNi_2$) in the α- and γ-phases, and fourteen $LaMgNi_2$ type interstices in the β-phase (see Table 2). Only some of these interstices are available for hydrogen occupancy, such as one type of Ni_4 tetrahedra in the α-phase (sites 4d) and another type in the γ-phase (sites 4b), and one out of three types of $LaNi_3$ tetrahedra (but none of the $MgNi_3$ type) in the β-phase.

As to the $LaMgNi_2$ type tetrahedra in the β- and γ-phases, they can be considered to be condensed into La_2MgNi_2 and $LaMg_2Ni_2$ type trigonal bi-pyramids of which only the former are available for hydrogen filling (see D1 situated between sites $4b_6$ and $4b_7$, and D2 between two $4b_3$ sites as shown in Table 2 and Fig. 3).

Finally, in contrast to C15 type metal–hydrogen systems, two H sites become completely void at increasing hydrogen concentrations, *i.e.* a Ni_4 site at the $\alpha-\beta$ and a $LaNi_3$ site at the $\beta-\gamma$ transition. Such hydrogen induced H site depopulations are unexpected and constitute a relatively rare phenomenon in metal–hydrogen systems. Only few other examples have been reported so far, such as the depopulation of Ho_6 interstices in the $Ho_6Fe_{23}-H$ system [20], of La_4Pd_2 interstices in the La_3Pd_5Si-H system [21], of $ErCo_3$ interstices in the $ErCo_3-H$ system [22], and of $(Ti,Zr)_4$ type interstices in the $Ti_{0.64}Zr_{0.36}Ni-H$ system [23]. Partial H site depopulations are more common, such as those of $Ce_2(Mn,Al)_2$ interstices in the $CeMn_{1.5}Al_{0.5}-H$ [24] and $CeMn_{1.8}Al_{0.2}H_{4.4}-H$ systems [25], and of $ErNi_3$ interstices in the $ErNi_3-H$ system [26], or the temperature induced depopulation of AB_3-type interstices at the benefit of A_2B_2-type interstices in the C15 type $TiZr_2-H$ system [27].

Some of these structural idiosyncrasies can be rationalized by atomic size considerations. Generally, only those metal interstices are considered suitable for hydrogen occupancy whose size exceeds a critical value (*e.g.* 0.40 Å, corresponding to the radius of the largest inscribed sphere [28]), and the bigger interstices are usually occupied first. On the other hand, the occupancy of such interstices may be prevented by other factors, such as repulsive H–H interactions originating from the proximity of other occupied

Table 2. Calculated hole sizes of tetrahedral interstices in α-, β- and γ-phases of $LaMgNi_4-D$ system. High-lighted cells refer to occupied D atom sites that are identical (4d site in α-phase, 4b site in γ-phase) or close to (all others) the centres of interstices derived by inscribing the largest sphere into the free space left by the coordinating metal atoms (r_{La} = 1.87 Å, r_{Mg} = 1.60 Å, r_{Ni} = 1.25 Å).

Interstitial site	Intermetallic		α			β			γ		
	Wyckoff site	Hole size (Å)	Wyckoff site	Hole size (Å)	Atom label	Wyckoff site	Hole size (Å)	Atom label	Wyckoff site	Hole size (Å)	Atom label
[Ni_4]	4b	0.30	4b	0.28		$2a_1$	0.30		4b	0.34	D2
	4d	0.32	4d	0.38	D1	$2a_1$	0.49		4d	0.49	
[$LaNi_3$]	$16e_1$	0.29	$16e_1$	0.34		$2a_3$	0.43	D3 (r_h = 0.37 Å)	$16e_1$	0.44	
						$2a_6$	0.32				
						$4b_1$	0.45				
[$MgNi_3$]	$16e_2$	0.34	$16e_2$	0.35		$2a_4$	0.40		$16e_2$	0.43	
						$2a_5$	0.58				
						$4b_2$	0.34				
[$LaMgNi_2$]	$48h_1$	0.33	$48h_1$	0.34		$4b_3$	0.48	D2 on trig. bipyr. site (r_h = 0.46 Å)	$48h_1$	0.44	D1
	$48h_2$	0.33	$48h_2$	0.32		$4b_4$	0.40		$48h_2$	0.41	
						$4b_5$	0.36				
						$4b_6$	0.50	D1 on trig. bipyr. site (r_h = 0.49 Å)			
						$4b_7$	0.51				
						$4b_8$	0.35				
						$4b_9$	0.35				
						$4b_{10}$	0.51				
						$4b_{11}$	0.33				
						$4b_{12}$	0.36				
						$2a_7$	0.38				
						$2a_8$	0.32				
						$2a_9$	0.33				
						$2a_{10}$	0.54				

interstices. This has led to the assumption of a "minimum separation" between H atoms in metal–hydride structures (*e.g.* 2.1 Å [28]). While the assumptions of minimum hole size and minimum H–H separation have been validated for many (mainly metallic) metal-hydrogen systems, including C15 type AB_2–H systems, they have only little predictive value because the size of the interstices in the hydride and their separations are generally unknown, at least prior to structure determination. Furthermore, quite a few exceptions are known to exist with respect to the 0.40 Å and 2.1 Å limits, and the preferential H occupancy of "large" interstices. In the present $LaMgNi_4$–H system, for example, Ni_4 type interstices are occupied in the α- and γ-phases despite their relatively small hole sizes in both the H-free compound ($r_h = 0.32$ and 0.30 Å, respectively) and the hydrides (D1 in α-phase: $r_h = 0.38$ Å; D2 in γ-phase: $r_h = 0.34$ Å), and in spite of the presence of bigger interstices in the structures (up to $r_h = 0.34$ Å in the H-free compound, and up to $r_h = 0.49$ Å in the γ-phase, see Table 2). As to the 2.1 Å limit, its influence on H content and H distribution in the present system can be assessed from the distances between the H sites and the centres of closest interstices as summarized in Table 3. All distances between occupied interstices are >2.1 Å, *i.e.* repulsive H–H interactions are unlikely to limit the hydrogen capacity of the various phases, thus suggesting as upper phase limits for the α, β- and γ-phases one, four and seven H atoms/f.u., respectively. On the other hand, repulsive H–H interactions are likely to influence the non-occupancy of certain interstices. The Ni_4 interstices (site $2a_2$: $r_h = 0.49$ Å) in the β-phase, for example, are presumably not occupied because of their proximity to fully occupied La_2MgNi_2 and $LaNi_3$ type interstices (D1: D–D = 1.73 Å, D2: D–D = 1.60 Å and D3: D–D = 1.29 Å, see Table 3). This is presumably also true for the relatively large $MgNi_3$ interstices in the β-phase (site $2a_5$: $r_h = 0.58$ Å) that are not occupied because of their proximity to occupied La_2MgNi_2 and $LaNi_3$ interstices (D1: D–D ~1.60 Å; D2: D–D ~1.79 Å), and for the relatively large Ni_4 interstices in the γ-phase (site $4d$: $r_h = 0.49$ Å) that are not occupied because of their proximity to occupied La_2MgNi_2 interstices (D1: D–D ~1.82 Å, see Table 3). Taken together, these observations suggest that there are no interstices in the structure large enough for H occupation but that are empty because of repulsive H–H interactions. Finally, except for the Ni_4 interstices, the H atoms are generally not situated at the centres of the metal tetrahedra, in particular those in $LaMgNi_2$ type interstices that are shifted away by up to 0.23 Å in the β-phase (D1, D2) and by 0.40 Å in the γ-phase (D1) as can be seen in Table 3.

In conclusion, despite the obvious stereochemical role of minimum interstitial hole size and minimum H–H separation, the exact H atom distribution in the $LaMgNi_4$–H system, and most other metal-hydrogen systems, cannot be explained on purely geometrical grounds. There exist clearly other structure determining factors such as metal–hydrogen bond strengths as modelled within the co-called "imaginary binary hydride model" [29], or probability distributions of paired electron density [30], or directional metal-hydrogen bonding as found in complex transition metal hydrides [31]. Concerning the latter, it is interesting to note that the Ni atoms in the present system tend to have tetrahedral H atom configurations consistent with sp^3 bonding, similar to those in all other known Ni based complex metal hydrides. This aspect will be highlighted in a forthcoming publication.

Table 3. Distances between occupied D atom sites and centres of closest interstices having a hole size radius >0.4 Å in β-$LaMgNi_4D_{3.7}$ (space group $Pmn2_1$) and γ-$LaMgNi_4D_{4.85}$ (space group $F\bar{4}3m$). Only distances below 2.1 Å are listed.

Occupied site	Neighbor site (r_h > 0.4 Å)	Distance (Å)
β-phase		
D1	$4b_6$	0.17
	$4b_7$	0.23
	$4b_{10}$	1.33
	$2a_4$	1.40
	$2a_{10}$	1.42
	$4b_1$	1.47
	$2a_5$	1.60
	$2a_2$	1.73
D2	$4b_3$	0.23
	$4b_1$	1.35
	$4b_{10}$	1.55
	$2a_2$	1.60
	$2a_5$	1.79
D3	$2a_3$	0.17
	$4b_4$	1.03
	$2a_7$	1.19
	$2a_2$	1.29
	$4b_1$	1.69
	$2a_4$	1.72
γ-phase		
D1	$48h_1$	0.40
	$16e_1$	1.49
	$48h_2$	1.55
	$4d$	1.82
	$16e$	1.86
D2	$16e_2$	1.29
	$48h_2$	1.81

Acknowledgments. This work was supported by the Swiss National Science Foundation and the Swiss Federal Office of Energy.

References

[1] Kono, T.; Sakai, I.; Yoshida, H.; Inaba, T.; Yamamoto, M.; Takeno, S.: Hydrogen-absorbing alloy, electrode and secondary battery. US Patent US006214492B1 (2001) 14.

[2] Si, T.Z.; Zhang, Q.A.; Liu, N.: Investigation on the structure and electrochemical properties of the laser sintered $La_{0.7}Mg_{0.3}Ni_{3.5}$ hydrogen storage alloys. Intl. J. Hydrogen Energy **33** (2008) 1729–1734.

[3] Dong, X.; Lu, F.; Zhang, Y.; Yang, L.; Wang, X.: Effect of La/Mg on the structure and electrochemical performance of La-Mg-Ni system hydrogen storage electrode alloy. Mater. Chem. Phys. **108** (2008) 251–256.

[4] Ozaki, T.; Kanemoto, M.; Kakeya, T.; Kitano, Y.; Kuzuhara, M.; Watada, M.; Tanase, S.; Sakai, T.: Stacking structures and electrode performances of rare earth-Mg-Ni-based alloys for advanced nickel-metal hydride battery. J. Alloy Compds **446/447** (2007) 620–624.
[5] Zhang, S.; Zhou, H.; Wang, Z.; Zou, R.P.; Xu, H.: Preparation and electrode properties of $NdMgNi_{4-x}Co_x$ hydrogen storage alloys. J. Alloy Compds **398** (2005) 269–271.
[6] Yvon, K.; Renaudin, G.; Wei, C.M.; Chou, M.Y.: Hydrogenation-Induced Insulating State in the Intermetallic Compound $LaMg_2Ni$. Phys. Rev. Lett. **94** (2005) 066403–4.
[7] Chotard, J.-N.; Filinchuk, Y.; Revaz, B.; Yvon, K.: Isolated $[Ni_2H_7]^{7-}$ and $[Ni_4H_{12}]^{12-}$ Ions in $La_2MgNi_2H_8$. Angew. Chem. Intl Ed. **45** (2006) 7770–7773.
[8] Geibel, C.; Klinger, U.; Weiden, M.; Buschinger, B.; Steglich, F.: Magnetic properties of new Ce–T–Mg compounds (T = Ni, Pd). Phys. B **237–238** (1997) 202–204.
[9] Kadir, K.; Noréus, D.; Yamashita, I.: Structural determination of $AMgNi_4$ (where A = Ca, La, Ce, Pr, Nd and Y) in the $AuBe_5$ type structure. J. Alloy Compds **345** (2002) 140–143.
[10] Guénée, L.; Favre-Nicolin, V.; Yvon, K.: Synthesis, crystal structure and hydrogenation properties of the ternary compounds $LaNi_4Mg$ and $NdNi_4Mg$. J. Alloy Compds **348** (2003) 129–137.
[11] Bobet, J.-L.; Lesportes, P.; Roquefere, J.-G.; Chevalier, B.; Asano, K.; Sakaki, K.; Akiba, E.: A preliminary study of some „pseudo-AB_2" compounds: $RENi_4Mg$ with RE=La, Ce and Gd. Structural and hydrogen sorption properties. Intl J. Hydrogen Energy **32** (2007) 2422–2428.
[12] Boultif, A.; Louer, L.: Dicvol04. J. Appl. Crystallogr. **37** (2004) 724–731.
[13] Favre-Nicolin, V.; Černý, R.: FOX, 'free objects for crystallography': a modular approach to ab initio structure determination from powder diffraction. J. Appl. Crystallogr. **35** (2002) 734–743.
[14] Rodriguez-Carvajal, J.: Recent advances in magnetic structure determination by neutron powder diffraction. Phys. B **192** (1993) 55.
[15] Aono, K.; Orimo, S.; Fujii, H.: Structural and hydriding properties of $MgYNi_4$: A new intermetallic compound with C15b-type Laves phase structure. J. Alloys Compds **309** (2000) L1–L4.
[16] Percheron-Guégan, A.; Lartigue, C.; Achard, J.C.: Correlations between the structural properties, the stability and the hydrogen content of substituted $LaNi_5$ compounds. J. Less-Common Met. **109** (1985) 287–309.
[17] Ivey, D.; Northwood, D.: Hydrogen site occupancy in AB_2 Laves phases. J. Less-Common Met. **115** (1986) 23–33.
[18] Gingl, F.; Yvon, K.; Vogt, T.; Hewat, A.: Synthesis and crystal structure of tetragonal $LnMg_2H_7$ (Ln = La, Ce), two Laves phase hydride derivatives having ordered hydrogen distribution. J. Alloys Compds **253/254** (1997) 313–317.
[19] Kohlmann, H.; Werner, F.; Yvon, K.; Hilscher, G.; Reissner, M.; Cuello, G. J.: Neutron Powder Diffraction with ^{nat}Sm: Crystal Structures and Magnetism of a Binary Samarium Deuteride and a Ternary Samarium Magnesium Deuteride. Chem. Eur. J. **13** (2007) 4178–4186.
[20] Rhyne, J.J.; Hardman-Rhyne, K.; Smith, H.K.; Wallace, W.E.: Deuterium site occupation and magnetism in $Ho_6Fe_{23}D_x$ compounds. J. Less-Common. Met. **94** (1983) 95–105.
[21] Tokaychuk, Y.O.; Filinchuk, Y.E.; Sheptyakov, D.V.; Yvon, K.: Hydrogen Absorption in Transition Metal Silicides: La_3Pd_5Si-Hydrogen System. Inorg. Chem. **47** (2008) 6303–6313.
[22] Filinchuk, Y.E.; Yvon, K.: Directional metal-hydrogen bonding in interstitial hydrides. III. Structural study of $ErCo_3D_x$ ($0 \leq x \leq 4.3$). J. Solid State Chem. **179** (2006) 1041–1052.
[23] Cuevas, F.; Latroche, M.; Bourée-Vigneron, F.; Percheron-Guégan, A.: A conjoint XRD-ND analysis of the crystal structures of austenitic and martensitic $Ti_{0.64}Zr_{0.36}Ni$ hydrides. J. Solid State Chem. **179** (2006) 3295–3307.
[24] Gross, K.J.; Chartouni, D.; Fauth, F.: A new hexagonal Laves phase deuteride $CeMn_{1.5}Al_{0.5}D_x$ ($0 < x < 4$) investigated by in situ neutron diffraction. J. Alloy Compds **306** (2000) 203–218.
[25] Filinchuk, Y.E.; Sheptyakov, D.; Hilscher, G.; Yvon, K.: Hydrogenation induced valence change and metal atom site exchange at room temperature in the C14-type sub-structure of $CeMn_{1.8}Al_{0.2}H_{4.4}$. J. Alloy Compds **356–357** (2003) 673–678.
[26] Filinchuk, Y.E.; Yvon, K.: Directional metal-hydrogen bonding in interstitial hydrides: I. Structural study of $ErNi_3D_x$ ($0 \leqq x \leqq 3.75$). J. Alloy Compds **404–406** (2005) 89–94.
[27] Tokaychuk, Y.; Keller, L.; Yvon, K.: Deuterium site energy difference in $ZrTi_2D_{4.3}$ as studied by high-temperature neutron diffraction. J. Alloy Compds **394** (2005) 126–130.
[28] Westlake, D.G.: Hydrides of intermetallic compounds: a review of stability, stoichiometry and preferred hydrogen sites. J. Less-Common Met. **91** (1983) 1–20.
[29] Jacob, I.; Bloch, J.M.; Shaltiel, D.; Davidov, D.: On the occupation of interstitial sites by hydrogen atoms in intermetallic hydrides: A quantitative model. Solid State Commun. **35** (1980) 155–158.
[30] Vajeeston, P.; Ravindran, P.; Vidya, R.; Kjekshus, A.; Fjellvåg, H.: Site preference of hydrogen in metal, alloy, and intermetallic frameworks. Europhys. Lett. **72** (2005) 569.
[31] Yvon, K.: Complex Transition Metal Hydrides. In: *Hydrogen as a Future Energy Carrier.* Wiley-VCH, 2007.